

Lack of Precursory Slip to the Hector Mine Earthquake as constrained by INSAR

by Robert J. Mellors, Lydie Sichoix, and David T. Sandwell

Abstract. We look for evidence of interseismic strain occurring between 1992 Landers event and the 1999 Hector Mine event near the Lavić Lake and Bullion faults using INSAR. Interferograms covering the Hector Mine epicentral region are studied for possible slip along the Bullion and Lavić Lake faults using both visual inspection and a matched filter technique intended to emphasize slip located at the nucleation point. Some indications of possible deformation associated with the July 5, 1992 M_L 5.4 Pisgah event is observed but high decorrelation prevents a conclusive determination. We see no evidence for precursory slip in the epicentral region up to 30 days before the Hector Mine event. We estimate that slip equivalent to a magnitude 4.5 event would have been observable in the months prior to the Hector Mine event and this places an upper bound on the long-term precursory slip, had it occurred. We note that INSAR is well suited for detecting precursory slip in general due to the high spatial resolution and the lack of ground instrumentation required, but that the detection level depends on the depth and orientation of the slip.

Introduction. The M_w 7.3 1992 Landers and M_w 7.1 1999 Hector Mine, California earthquakes occurred 20 km and 7 years apart as part of a cluster of events that also included the 1992 Joshua Tree and Big Bear events (Figure 1). The recurrence time in this area is usually measured in thousands of years (Rockwell et al., 2000). This suggests that the Hector Mine event was perhaps "triggered" by the earlier Landers event (Parsons and Dreger, 2000; Freed and Lin, 2001). These connections are emphasized by the fact that several Landers aftershocks (including the 1992 M_L

5.4 Pisgah event) occurred very near the eventual nucleation site of the Hector Mine event. The Hector Mine event itself was preceded by 12 foreshocks with magnitudes between $M_L 1.9$ and $M_L 3.8$.

A significant question is: is this stretch of fault at the Hector Mine rupture different from other faults nearby? Is it physically different? Or was the rupture simply a small event that happened, through a random combination of favorable stresses and fault geometries, to grow into a large rupture? As the basic earthquake process is largely unknown, it is useful to constrain these events with all available data. In this study we look for any evidence of aseismic strain along the Lavic Lake and Bullion faults between the Landers and Hector Mine events. While such slip might seem unlikely, it should be noted that it has not been possible previously to make high resolution strain measurements at the epicentral region of a large earthquake prior to the event. The existence of repeated Landers aftershocks and Hector Mine foreshocks suggests higher strain rates. We are providing bounds on any long-term precursory slip, which has implications for the nucleation process of large earthquakes.

Precursory slip near the nucleation point is an important feature of many laboratory and theoretical models of earthquakes (Dieterich and Kilgore, 1996; Ohnaka, 1996; Scholtz, 1990). There are indications that the size of the slip might scale to the size of the resulting earthquake, which would be critical for use as a prediction tool. However, the amount of premonitory slip appears to depend strongly on the fault geometry and material properties such as surface roughness, gouge thickness, gouge particle size, and pore pressure. As these parameters are poorly known in nature it is impossible to predict from existing data whether precursory slip exists or is observable for earthquakes.

Unambiguous observational support of precursory slip is lacking. There are historical reports of uplift or subsidence preceding some great earthquakes (Rikitake, 1975; Mogi, 1985), sometimes by several weeks. On a shorter time scale, there are also reports of both slow slip (Ihmle and Jordan, 1994) and rapid slip (Kanamori and Cipar, 1974; Beroza and Ellsworth, 1996; Iio, 1995) immediately before some large events. Unfortunately, despite the deployment of a variety of instrumentation including both strainmeters and geodetic instruments, no robust and reliable measurements of precursory strain have been reported (Takemoto, 1991). For example, borehole strainmeters located only 37 km from the epicenter of the 1989 Ms 7.1 Loma Prieta earthquake failed to show any precursory slip (Johnston et al., 1990). It was estimated that slip equivalent to a magnitude 5 earthquake would have been detected. Such reported features as ground water level changes (Lomnitz, 1994), increased radon emissions (Trique et al., 1999), and electromagnetic emissions (Fraser-Smith et al., 1990) may reflect increased strain and/or volume change in the epicentral region related to the earthquake process. The time scale is usually weeks to days (12 days for the ULF anomaly associated with the 1989 Loma Prieta earthquake).

Reliable observations of precursory slip are hampered by the need for measurements to be made near the site of nucleation, which requires that the instruments must be deployed (or measurements conducted) very near the site of the epicenter prior to the earthquake. This is difficult, as the epicentral location and time of large earthquakes is unknown beforehand. Even when the 1989 Loma Prieta earthquake occurred along a relatively well-instrumented section of fault, the lower detection limit was the equivalent of an M 5.3 earthquake (Johnston et al., 1990). Consequently, no high-resolution measurements have been made at the epicenter of a large earthquake prior to the event as far as we know. The advent of interferometric synthetic aperture radar (INSAR) has changed this, as it allows sensitive strain measurements to be made over a

wide area without pre-existing instrumentation or ground measurements. Therefore INSAR presents an opportunity to monitor surface strain at a high resolution at the nucleation site of a major event before it occurs.

INSAR has several disadvantages. One is poor temporal resolution due to the fixed repeat cycle (35 days for ERS-2, for example). If significant slip only occurs on the scale of days or hours before an event, then repeat data must be collected (and processed) more frequently to increase the likelihood of catching an event. Due to the geometry of acquisition, the nucleation of events with a significant vertical component (i.e. thrust or normal events) would be more likely to be measurable than strike-slip events, assuming that the nucleation slip follows a similar mechanism as the major event.

Method. Both the Landers and Hector Mine events were well-recorded by INSAR as well as GPS and other data (Massonet et al., 1993; Peltzer et al., 1994; Zebker et al. 1994; Shen et al., 1994; Price and Sandwell, 1998; Sandwell et al., 1998; Sandwell et al., 2000; Hurst et al., 2000). In addition to the rupture along the main trace a variety of other co-seismic and post-seismic deformations were observed. Triggered slip occurred on many of the neighboring faults (Bodin et al., 1994; Hart et al., 1993; Peltzer et al, 1994; Price and Sandwell, 1999) and several different types of post-seismic deformation were noted including afterslip as well as longer wavelength features attributed to a combination of mechanisms including viscous flow in the upper mantle, poroelastic rebound and fault-zone collapse (Massonet et al, 1994; Massonet et al, 1996; Savage and Svarc, 1997; Pelzer et al, 1998; Pollitz et al., 2000).

Several ERS satellite tracks, both ascending and descending, cross the area, and we have a wide variety of possible interferograms. As the Hector Mine events occurred near (within 30

km and seven years) of the 1992 Landers events, we used a variety of ERS SAR data between the two events as well, with emphasis on the area near the epicenter of the Hector Mine event. The Mojave Desert in particular is an excellent site for INSAR as it generally possesses high correlation, low atmospheric humidity and a high-resolution accurate digital elevation model is readily available. We examine the differential phase images for evidence of strain between the two events and especially for strain near the time of the Hector Mine earthquake. The images are analyzed both visually and using a matched filter technique in an attempt to improve the signal to noise ratio.

We use C band (5.66 cm) data from the ERS-1 and ERS-2 satellites (Figure 1 and Table 1). The data were acquired through the WINSAR program and through a downlink at the Scripps Institute of Oceanography. SAR processing was performed using a range-doppler algorithm as part of the SIOSAR (Price, 1997) package. Standard INSAR processing was conducted using precise orbits (Scharoo and Visser, 1998) and a combination of a 90 m USGS DEM and a tandem pair to eliminate topography effects.

Available INSAR data (Table 1) include a number of scenes from several tracks spanning the time between the Landers and Hector Mine events. Both ascending and descending data was used, although coverage of the faults varied between tracks. We concentrated on the scenes nearest the time of the Hector Mine rupture, and with as favorable a baseline as possible to increase coherence and decrease topographic effects. We focused on pairs that included one scene near the time of the earthquake but we also calculated interferograms to span much of the period between the Landers and Hector Mine events to check for any other slip in the area. The earliest interferogram begins 5 days after Landers and shows post-seismic Landers deformation as reported in previous studies.

Pisgah earthquake. On 5 July 1992 an M_L 5.4 event occurred near the Pisgah fault. Several focal mechanisms based on first-motions and waveform modeling were available (Hauksson, 2000; Zhu and Helmberger, 1996; Thio and Kanamori, 1995). Both Hauksson (2000) and Thio and Kanamori (1995) suggested a shallow epicenter while the Zhu and Helmberger (1996) indicated a depth of 9.6 km (Table 1). Modeling using these parameters along with a slip of 0.2 m on a square fault 3.7 km wide indicated that the event should be visible but unfortunately the area was highly decorrelated on both scenes and only patches of phase were present (Figure 2). The model was shifted to allow a better visual fit to the data and the center point of the fault model is 0.5 km east and 0.7 km south of the Hauksson (2000) epicenter. The model presented here places the bottom of the fault at a depth of 5 km. Models with shallower depths resulted in a higher fringe rate. We tried a variety of methods to unwrap the interferogram and show results from a quality-guided method (Ghiglia and Romero, 1998) although due to the noise and patches of isolated phase it is not a unique solution. The amplitudes of the data are roughly comparable to the expected signal but the high decorrelation and noise made it impossible to clearly distinguish signal, if any, from noise. Examination of the area on a second interferogram showed a similar pattern, suggesting that it is not caused by atmospheric effects. Comparison of the wrapped phase with the modeled results was also inconclusive. The area of high decorrelation matched the area of maximum deformation although the deformation should not have been sufficient to create decorrelation unless there was surface rupture. The only clear conclusion is that the event appears at the limit of detection for this data.

We also tried applying a matched filter based on the expected source to test whether this could be used to improve the resolution. The matched filters were constructed using an assumed

source and then cross-correlated with the data. Deformation was modeled using the program *rngchn* (Feigl and Dupre, 1997). Both unwrapped and phase gradient version of the data and signal were tested. Matched filter results from the unwrapped data were further normalized to reduce peaks associated with high pixel values. We tested this technique using synthetic data with added noise and on another M_L 5.4 Landers aftershock (Feigl et al., 1995) located on the same scene and with a known focal mechanism, depth, and magnitude. This event was detected successfully (i.e. produced a global maximum). Unfortunately, application to the Pisgah event using a mechanism based on the seismic data did not result in detection, possibly due to high noise or poor signal match.

Search for aseismic slip. An examination of the scenes prior to the Hector Mine event fails to show any obvious deformation in the area of the Lavic Lake/Bullion faults (Figure 3). Variations in phase are visible but are not clearly associated with the fault. These are likely due to atmospheric variations. The variations show a weak correlation with topography, possibly due to atmospheric phase delays related to topography (e.g. Delacourt et al., 1998). Very long wavelength variations may be due to orbital errors. Following visual examination and construction of cross-sections, we attempted to increase the sensitivity of measurement from the pairs closest in time to the earthquake in several ways. The first method was by simply stacking the unwrapped phase from scenes on track 399 to improve the signal and reduce atmospheric effects. No improvement was visible.

We again applied a variety of matched filters in an effort to detect subtle signals not easily visible. Filters were constructed to detect strain at the surface and at a depth of 5 km, the depth of the Hector Mine hypocenter ($5 \text{ km} \pm 3$). Fault orientation was taken from the first

motion focal mechanism (Hauksson, 2000) which presumably reflects the orientation of the initial rupture (and assuming slip on the northwest/southeast striking plane). The shape and magnitude of the potential nucleating slip is unknown, so we used a square fault with the slip scaled to the fault dimensions by 1×10^{-5} (while seismic slip generally scales with fault size, it is not clear that this is true for aseismic precursory slip) (Figure 2). This is equivalent to a M_L 4.5 event. As INSAR measures only line-of-sight motion, the geometry is not favorable for a strike-slip event at depth. We estimate that the nucleation zone must be at least 2km square centered at 5 km to show a clear signal. Shallower signals will be easier to detect but deeper ones will require more slip. It should be noted that the cumulative surface deformation would be measured. Again, the application of the matched filter did not produce an increased signal near the epicentral site.

Conclusions. Examination of scenes covering the period between the Landers and Hector Mine earthquakes did not reveal any precursory slip that occurred in the time up to 30 days previous to the event. The results are perhaps not too surprising but we do show that INSAR detection levels are comparable to the best observations and constraints provided by other means. Tests with synthetic data and white noise indicates that the detection level would have been easily sufficient to observe a slip roughly equivalent to a magnitude 4.5 earthquake at a depth of 5 km. For scenes with more realistic noise characteristics and decorrelation such as those spanning the Pisgah event it appears the detection level is higher (at least M_L 5.4).

Acknowledgements. This study depended on Synthetic Aperture Radar data provided by the European Space Agency through their North American distributors, Eurimage and SpotImage. Data were purchased by the WInSAR consortium with funding from NASA, NSF and USGS.

Department of Geological Sciences, San Diego State University
San Diego CA 92182
(R.J.M)

Institute of Geophysics and Planetary Physics,
Scripps Institute of Oceanography
San Diego CA 92122
(L. S. and D. T. S.)

References:

- Behr, J., R. Bilham, P. Bodin, and S. Gross, (1994), Eureka Peak afterslip following the 28 June 1992 Landers earthquake, *Bull. Seismo. Soc. Amer.*, **84**, 826-834.
- Beroza, G.C. and W.L. Ellsworth, (1996) Properties of the seismic nucleation phase, *Tectonophysics*, **261**, 209-227.
- Bodin, P. R. Bilham, J. Behr, J. Gomberg, and K. W. Hudnut, 1994, Slip triggered on Southern California faults by the 1992 Joshua Tree, Landers, and Big Bear earthquakes, *Bull. Seismo. Soc. Amer.*, **84**, 806-816.
- Delacourt, C., P. Briole, and J. Achache, Tropospheric correction of SAR interferograms with strong topography: Application to Etna, (1998), *Geophys. Res. Lett.*, **25**, 2849-2852.
- Dieterich, J. H. and B. Kilgore, (1996), Implications of fault constitutive properties for earthquake prediction, *Proc. Natl. Acad. Sci.*, **93**, 3795-3802.
- Feigl, K.L., A. Sargent, A. and D. Jacq, (1995), Estimation of an earthquake focal mechanism from a satellite radar interferogram: Application to the December 4, 1992 Landers aftershock. *Geophys. Res. Lett.*, **22**, 1037-1040.
- Feigl, K. L. and E. Dupre, (1998), RNGCHN: a program to calculate displacement components from dislocations in an elastic half-space with applications for modeling geodetic measurements of crustal deformation, *Computers and Geosciences*, **25**, 695-704.
- Fraser-Smith, A.C., A. Bernardi, P.R. McGill, M.E. Ladd, R.A. Helliwell, and O.G. Villard, Jr., (1990), Low-frequency magnetic field measurements near the epicenter of the Ms 7.1 Loma Prieta earthquake, *Geoph. Res. Letts.*, **17**, 1465-1468.
- Freed, A. M. and J. Lin, (2001), Delayed triggering of the 1999 Hector Mine earthquake by viscoelastic stress transfer, *Nature*, **411**, 180-183.
- Ghiglia, D. C. and M. D. Pritt, (1998), *Two-dimensional phase unwrapping: Theory, algorithms, and software*, John Wiley and Sons, Inc. 493 p.
- Hauksson, E., (2000) Crustal structure and seismicity distribution adjacent to the Pacific and North America plate boundary in Southern California, *J. Geophys. Res.*, **105**, 13875-13903.
- Hart, E. W., W. A. Bryant, and J. A. Treiman, (1993), Surface faulting associated with the June 1992 Landers earthquake, California, *Calif. Geol.*, **46**, 10-16.
- Hurst, Kenneth J., D. F. Argus, A. Donnellan, M. B. Heflin, D. C. Jefferson, G. A. Lyzenga, J. W. Parker, M. Smith, F. H. Webb, J. F. Zumberge (2000), The coseismic geodetic signature of the 1999 Hector Mine Earthquake, *Geophys. Res. Lett.*, **27**, 2733-2736.
- Ihmle, P. F. and T. H. Jordan, (1994), Teleseismic search for slow precursors to large earthquakes, *Science*, **266**, 1547-1551.
- Iio Y., (1995). Observations of the slow initial phase generated by micro-earthquakes: Implications for earthquake nucleation and propagation , *J. Geophys. Res.*, **100**, 15333-15349.
- Johnston, M. J. S., A. T. Linde, and M. T. Gladwin, (1990), Near-field high resolution strain measurements prior to the October 18, 1989, Loma Prieta Ms 7.1 earthquake, *Geophys. Res. Lett.*, **17**, 1777-1780.
- Kanamori, H. and J. Cipar, (1974), Focal processes of the Great Chilean earthquake of May 22, 1960, *Physics of the Earth and Planet. Int.*, **9**, 128-136.
- Lomnitz, C., (1994), *Fundamentals of earthquake prediction*, John Wiley & Sons, Inc., New York, pp 325.

- Massonnet, D., Rossi, M., Carmona, C., Adragna, F., Peltzer, G., Feigl, K., Rabaut, T., (1993), The displacement field of the Landers earthquake mapped by radar interferometry, *Nature*, **364**, 138-142.
- Massonnet, D., W. Thatcher, and H. Vadone, (1996), Detection of postseismic fault-zone collapse following the Landers earthquake, *Nature*, **382**, 612-615.
- Massonnet, D., Feigl, K., Rossi, M. and Adragna, F., (1994), Radar interferometric mapping of deformation in the year after the Landers earthquake. *Nature*, **369**, 227-230.
- Mogi, K. 1985, Earthquake prediction, Academic Press, 33 pp.
- Ohnaka, M., Nonuniformity of the constitutive law parameters for shear rupture and quasistatic nucleation to dynamic rupture: A physical model of earthquake generation process, (1996), *Proc. Natl. Acad. Sci.*, **93**, 3795-3802.
- Parsons, T., and D. S. Dreger, (2000). Static-stress impact of the 1992 Landers earthquake sequence on nucleation and slip at the site of the 1999 M=7.1 Hector Mine earthquake, southern California, *Geophys. Res. Lett.*, **27**, 1949-1952.
- Peltzer, G., Hudnut, K.W. and Feigl, K.L., (1994), Analysis of coseismic surface displacement gradients using radar interferometry: New insights into the Landers earthquake. *J. of Geophys. Res.*, **99**, 21971-21982.
- Peltzer, G., P. Rosen, F. Rogez, and K. Hudnut, (1998), Poroelastic rebound along the Landers 1992 earthquake surface rupture, *J. Geophys. Res.*, **103**, 30131-30145.
- Pollitz, F. F., G. Peltzer, and R. Burgmann, (2000), Mobility of continental mantle: Evidence from postseismic geodetic observations following the 1992 Landers earthquake, *J. Geophys. Res.*, **105**, 8035-8054.
- Price, E., (1997) Coseismic and Postseismic Deformations Associated With the 1992 Landers, California, Earthquake Measured by Synthetic Aperture Radar Interferometry Ph. D thesis, University of California, San Diego, 159 pages.
- Price, E. and D. Sandwell, (1998), Small-scale deformation associated with the 1992 Landers, California earthquake mapped by SAR interferometry, *J. Geophys. Res.*, **103**, 27001-27016.
- Richards-Dinger, K. B. and P. M. Shearer, Earthquake locations in Southern California obtained using source-specific station terms, (2000), *J. Geophys. Res.*, **105**, 10939-10960.
- Rikitake, T. Earthquake precursors, (1975), *Bull. Seismo. Soc. Amer.*, **65**, 1133-1162.
- Rockwell, T. K., S. Lindvall, M. Herzberg, D. Murbach, T Dawson, and G Berger, 2000, Paleoseismology of the Johnson Valley, Kickapoo, and Homestead Valley Faults: Clustering of earthquakes in the Eastern California Shear zone, (2001), *Bull. Seismo. Soc. Amer.*, **90**, 1200-1236.
- Sandwell, D. T. and E. J. Price, (1998), Phase gradient approach to stacking interferograms, *J. Geophys. Res.*, **103**, 30183-30204.
- Sandwell, David T., L. Sichoix, D. Agnew, Y. Bock, J-B. Minster, (2000), Near real-time radar interferometry of the Mw 7.1 Hector Mine Earthquake, *Geophys. Res. Lett.* **27**, 3101-3104.
- Savage, J. C. and J. L. Svarc, (1997), Postseismic deformation associated with the 1992 Mw=7.3 Landers, earthquake, southern California, *J. Geophys. Res.*, **102**, 7565-7577.
- Scharroo, R. and P. Visser, (1998), Precise orbit determination and gravity field improvements for the ERS satellites, *J. Geophys. Res.*, **102**, 8113-8127.
- Scholtz, C. (1990), The mechanics of earthquakes and faulting, Cambridge University Press, 439 p.

Shen, Z-K., D. D. Jackson, Y. Feng, M. Cline, M. Kim, P. Fang, and Y. Bock, (1994), Postseismic deformation following the Landers earthquake, 1994, California, 28 June 1992, *Bull. Seismo. Soc. Amer.*, **84**, 780-791.

Takemoto, S., (1991), Some problems on detection of earthquake precursors by means of continuous monitoring of crustal strains and tilts, *J. Geophys. Res.*, **96**, 10377-10390.

Thio H. K., and H. Kanamori, (1995), Moment tensor inversions for local earthquakes using surface waves recorded at TERRAscope, *Bull. Seismo. Soc. Amer.* **85**, 1021-1038.

Trique, M., P. Richon, F. Perrier, J. P. Avouac, and J. C. Sabroux, (1999), Radon emanation and electric potential variations associated with transient deformation near reservoir lakes, *Nature*, **399**, 137-140.

Vidale, J. E., D. C Agnew, M. J. S. Johnston, and D. H. Oppenheimer, (1998), Absence of earthquake correlation with Earth tides: An indication of high pre-seismic fault stress rate, *J. of Geophys. Res.*, **103**, 24567-24572.

Zebker, H.A., Rosen, P.A., Goldstein, R.M., Gabriel, A. and Werner, C.L., (1994), On the derivation of coseismic displacement fields using differential radar interferometry: The Landers earthquake. *J. of Geophys. Res.*, **99**, 19617-19634.

Zhu, L. and Helmberger, D, V. (1996), Advancements in source estimation techniques using broadband regional seismograms, *Bull. Seismo. Soc. Amer.*, **86**, 1634-1641.

Table 1. List of SAR data. ERS 1 and 2 scenes examined in this study. Data acquired through the WINSAR consortium and courtesy of the European Space Agency.

Table 2. Source parameters. Parameters for the 21:18 5 July 1992 Pisgah event. In this study we used the strike, dip and rake of Hauksson (2000) with a slip of 0.2 m on a square fault 3.7 km wide. The base of the fault was at a depth of 5 km and the center point at 116.32 W, 34.57 N.

Figure 1. Map location of the Landers/Hector Mine earthquake region. Dots denote earthquakes smaller than Ml 4.0, diamonds are between magnitude 4 and 6, and stars denote large events greater than 7. The frame outlines of descending SAR tracks are shown as solid lines and dashed lines mark ascending tracks. Light lines indicate mapped faults and dashed where inferred.

Figure 2. Unwrapped interferogram (left) and modeled deformation (right), of the area near the July 1992 Pisgah event (epicenter marked by a star). Data is from the pair e1_05053-e1_08059. Solid gray indicates areas of no data due to correlation less than 0.2. Above the images are north-south and east-west cross sections of the data (dots) and model (line). Cross-sections are marked on the map view.

Figure 3. (Left) Interferogram of the epicentral region of the Hector Mine events spanning 3.45 years and up to 30 days before the Hector Mine event. Triangles mark "aftershocks" of the Landers event and the large star is the location of the Hector Mine event. (Right) Model of slip at the nucleation zone. Scale is in mm along line-of-sight to the satellite. Closed circles mark foreshocks (events occurring less than 1 month previous to the Hector Mine event).

Table 1. List of SAR data.

orbit	date	orbit	date	diff (years)	days prior HM	track	perp. base. (m)
e1_05053	1992 185	e1_08059	1993 029	0.57	1449	399D	126
e1_10063	1993 169	e2_21796	1999 172	6.01	117	399 D	-170
e1_21429	1995 232	e2_21796	1999 172	3.84	117	399 D	-49
e1_07558	1992 360	e2_22798	1999 242	6.68	47	399 D	-55
e1_11065	1993 239	e2_22798	1999 242	6.01	47	399 D	-54
e1_05053	1992 185	e1_19425	1995 092	2.75	1658	399 D	59
e2_04991	1996 094	e2_23027	1999 258	3.45	31	127 D	-145
e1_20105	1995 140	e2_22476	1999 220	4.22	69	077 A	-47

Table 2. Source parameters of the Pisgah aftershock.

<i>lat</i>	<i>lon(w)</i>	<i>strike</i>	<i>dip</i>	<i>rake</i>	<i>depth</i>	<i>magnitude</i>	<i>source</i>
34.58	116.32	75	75	170	1.14	M_L 5.4	Hauksson (2000)
34.58	116.32	190	50	60	1.14	M_L 5.4	Hauksson (2000)
34.58	116.32	76	72	34	1.1	Mw 5.3	Thio and Kanamori (1995)
34.58	116.32	73	64	33	9.6	Mw 5.2	Zhu and Helmberger (1996)

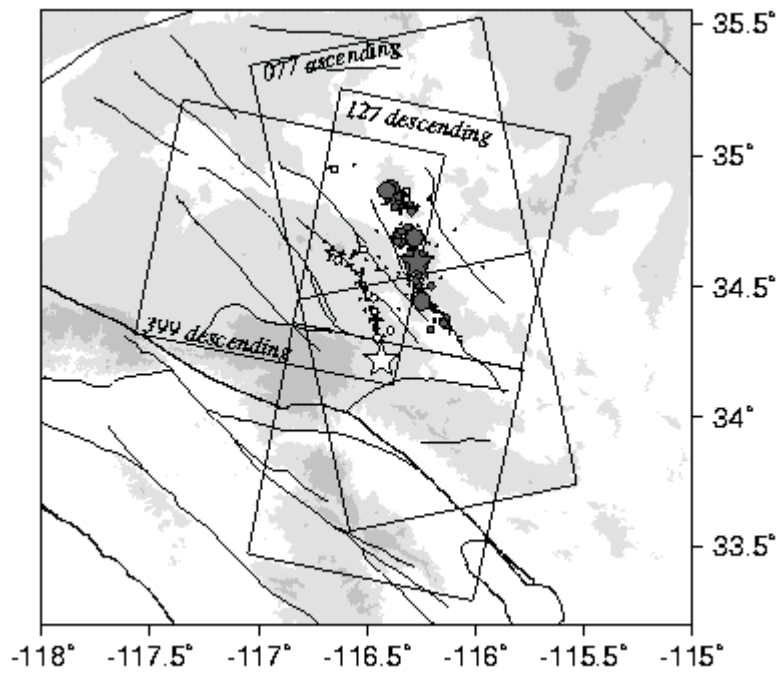


Figure 1.

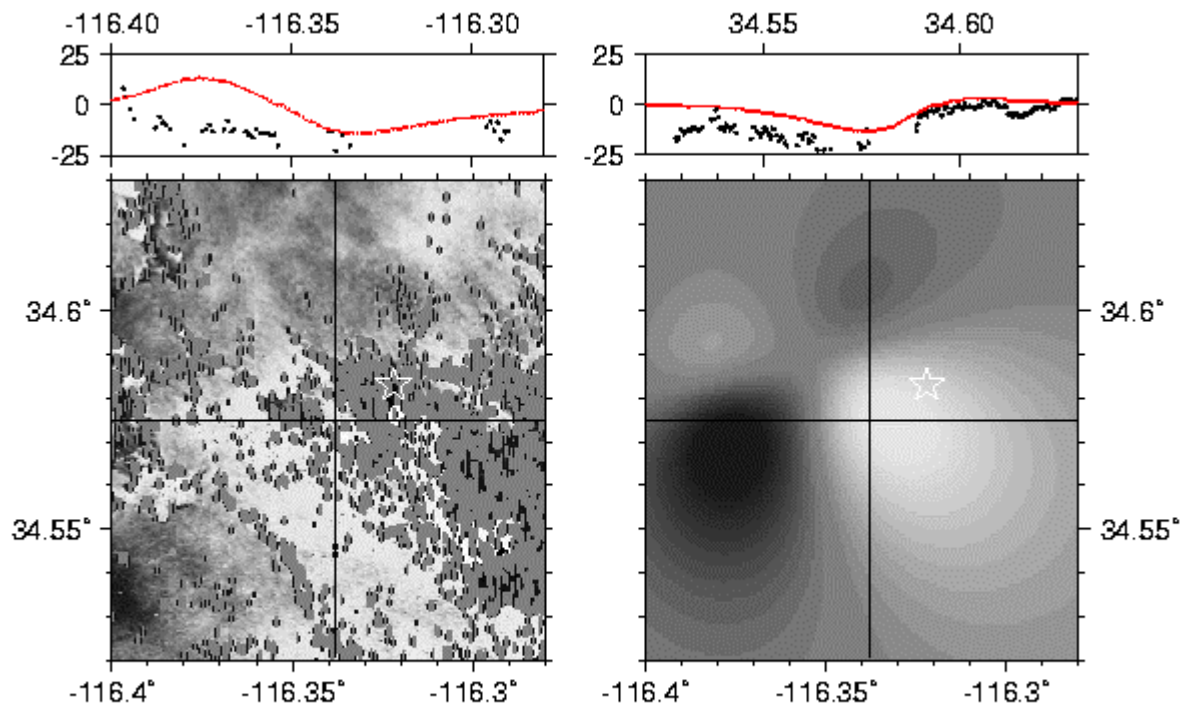
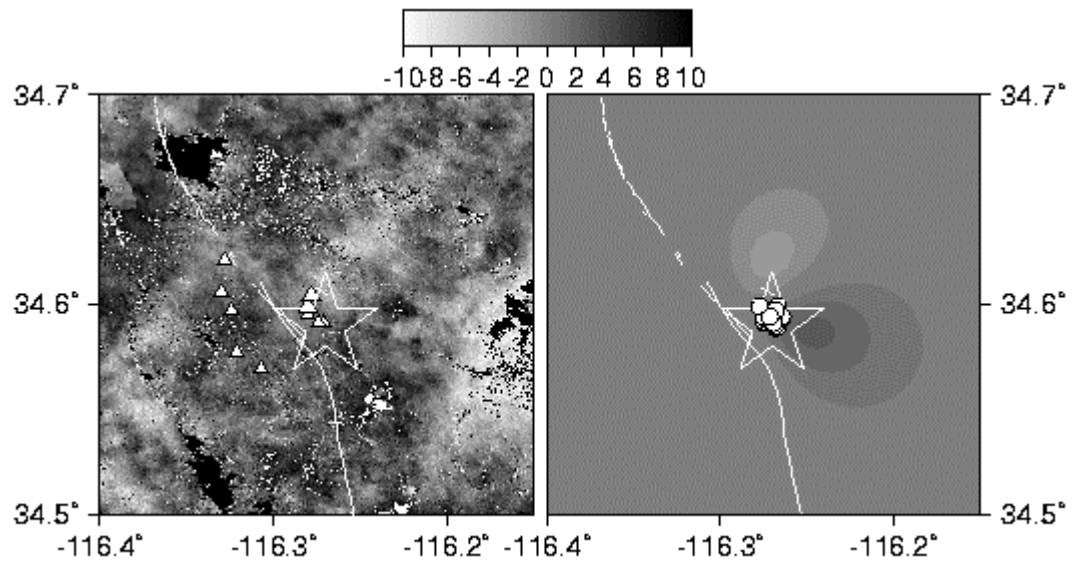


Figure 2.



Fig